Applying AI to Gain Insights Into the Novel Immune Checkpoint PVRIG Through Single-Cell and Spatial Transcriptomics

Roy Granit[1]*, Déborah Hayoun[1], Zoya Alteber[1], Sergey Nemzer[1], Assaf Wool[1], Katya Nikitskaya[1], Tal Brender[1], Amir Toporik[1], Amit Novik[1], Gady Cojocaru[1], Itamar Borukhov[1], Rob Foreman[2], Natalia Petrenko[2], Jiang He[2], Sudipto Ganguly[3], Drew Pardoll[3], Zurit Levine[1], Eran Ophir[1]

[1]Compugen LTD, Harokmim 26, Holon, Israel, [2]Vizgen Inc, Cambridge, MA, [3]Bloomberg-Kimmel Institute for Cancer Immunotherapy, Sidney Kimmel Comprehensive Cancer Center, Johns Hopkins University School of Medicine; Baltimore, MD, USA, *Corresponding Author royg@cgen.com

compugen
FROM CODE TO CURE®

Abstract # 2228812
Poster #40

Introduction

Background: Cancer immunotherapy has emerged as a groundbreaking treatment, yet its effectiveness remains limited. There is a significant need to identify new checkpoints and inhibitors to overcome immunotherapy resistance. We discovered PVRIG, a novel T-cell checkpoint based on the evolutionary conservation of genomic exon arrangement, and are evaluating COM701, a potential first-in-class anti-PVRIG antibody, in clinical studies. Our exploration revealed that PVRIG is not accurately detected in standard single-cell RNA sequencing assays due to a predicted read-through transcript that causes PVRIG reads to be discarded.

Methods: Both by generating a corrected reference genome, or training a deep-learning inference model, we captured accurate PVRIG expression levels. Using this reference, we conducted comprehensive analyses of single-cell RNA sequencing datasets and developed a unique, deep-learning based, dimension reduction strategy to highlight differences between largely-similar T-cell states. Using MERFISH, we analyzed Immune Aggregates (ImmuAg) structures, which hold predictive value for immunotherapy responses.

Findings: We found that PVRIG is uniquely expressed in stem-like memory T-cell populations (Tscm), which have strong proliferative capacity, while other T-cell checkpoints targeted by approved immunotherapies were more abundantly expressed on exhausted cells. PVRIG binds PVRL2 (NECTIN2) which is expressed on dendritic as well as tumor cells. Our findings show that PVRIG+CD28+CD8 Tscm predominantly localize within ImmuAg, interacting with PVRL2+LAMP3+dentritic cells. PVRIG blockade could therefore enhance the differentiation and expansion of Tscm, driving T-cell immunity even in less inflamed tumors. Together, these insights highlight the unique biology of PVRIG and suggest that its inhibition might induce anti-tumor activity in indications previously refractory to immunotherapy.

DNAM axis potential to be a game changer in the fight against cancer

- PVRIG and TIGIT discovered by Compugen's discovery platform
- DNAM axis – two parallel and complementary inhibitory pathways (PVRIG & TIGIT)
- Potential intersection between PVRIG/TIGIT and PD-1 pathway

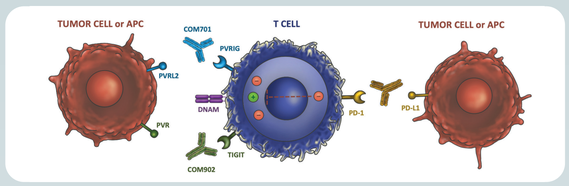

Support combination approach to overcome immunotherapy resistance

Discovery of PVRIG via evolutionarily conservation of genomic exon arrangement and recent confirmation using LLM

Employing our unique computational algorithms to define new members of the B7/CD28 family we identified PVRIG, as a potential novel immune checkpoint. More recently, we applied the ESM2 protein sequence Large Language Model (LLM) to all membrane genes and found that PVRIG clusters along other immune checkpoints.

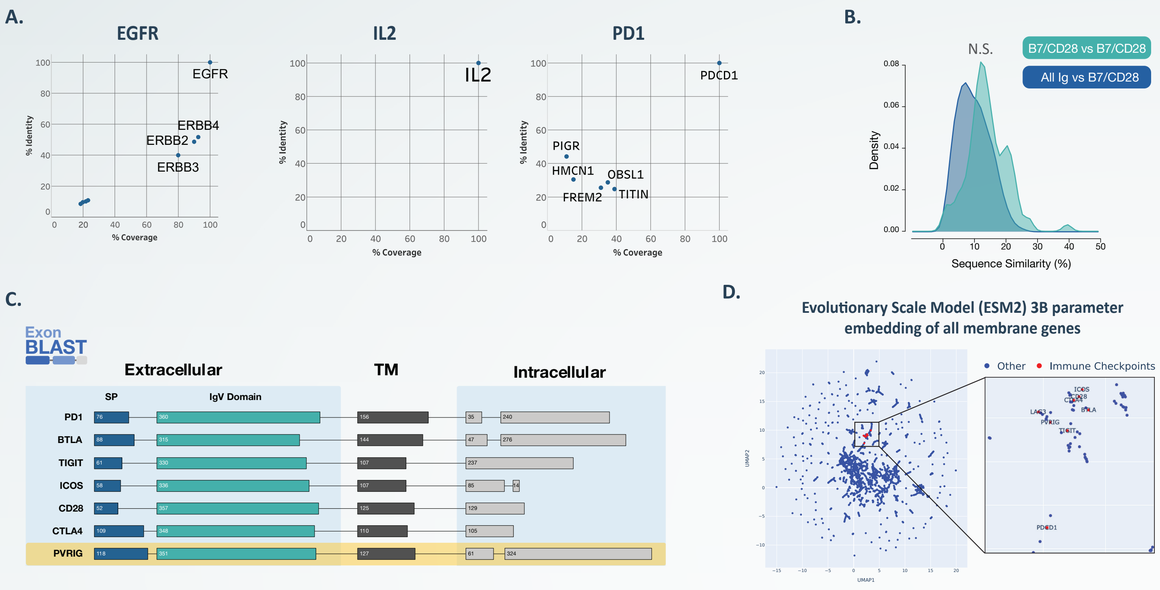

Identification of PVRIG using the Exon-Blast methodology. A. Plots illustrating the lower sequence conservation of immune-related genes (e.g., IL2 and PD1) compared to EGFR family members: This is indicative of evolutionary pressure exerted on immune genes. **B.** Histogram demonstrating that sequence similarity among B7/CD28 family members is not significantly greater than their similarity to Ig family genes: This further emphasizes the limited sequence conservation in immune genes. **C.** Output from the Exon-Blast algorithm reveals that exon size and arrangement are conserved among known immune checkpoints. This led to the discovery that PVRIG could potentially serve as one. **D.** UMAP showing the clustered embedding derived from the ESM2 3B model, which was applied on the AA sequences of all membrane proteins, immune checkpoints are colored in red. In the enlarged figure on the right, it can be seen that PVRIG clusters with other immune-checkpoints, supporting its initial discovery.

PVRIG is poorly detected in 10x Chromium data due to overlap with STAG3

We noted that in 10x Chromium datasets, PVRIG is poorly detected due to multi-mapping of reads to STAG3-209, a read-through transcript with poor support levels that was described only once in the literature and is not detected in 10x or PacBio long-read sequencing.

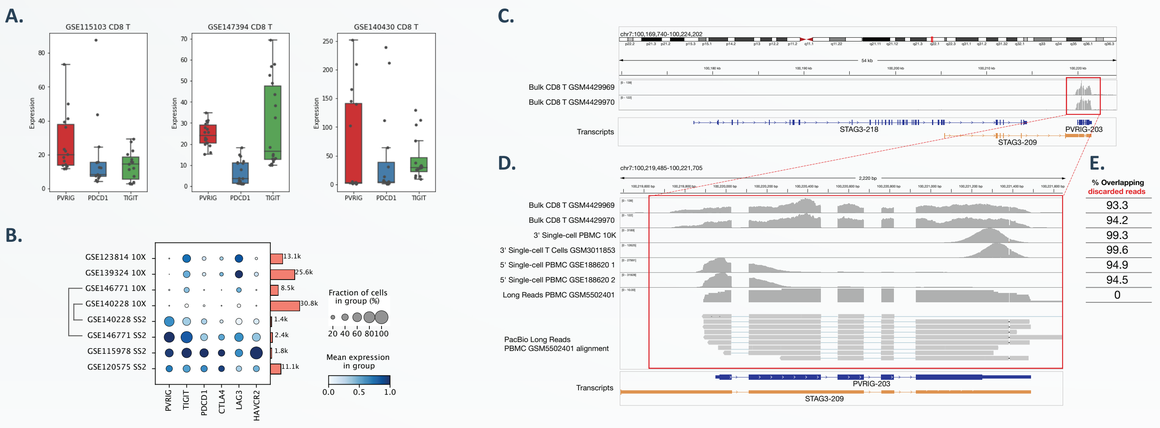

Unlike bulk and smart-seq PVRIG is poorly detected in 10x single cell data due to overlap with STAG3-209. A. Boxplots showing that PVRIG, TIGIT and PD-1 are expressed across several CD8 T-cell datasets as measured using bulk RNA-seq. GSE140430 isolated CD8 T-cells from TME, rest are from blood. **B.** Dotplot showing the expression of PVRIG and additional T-cell checkpoints in several Smart-seq2 (SS2) datasets (bottom) but PVRIG is not detected in 10x datasets (top). Line connect datasets from the same studies conducted with the two technologies. Bars indicate number of cells in each sample **C.** The STAG3-PVRIG genomic locus. Histograms feature the distribution of reads in bulk RNA-seq data of isolated CD8 T-cells highlighting that PVRIG is expressed in such cells (red box). Gene structures appear below in blue. **D.** Closer view of PVRIG locus. Histograms highlight the distribution of reads in the indicated datasets. **E.** Fraction of reads that map to both PVRIG and STAG3-209 and are thus discarded.

Corrected gene model as well as deep-learning model enables correct detection of PVRIG and validates expression in Tscm in ovarian tumor samples

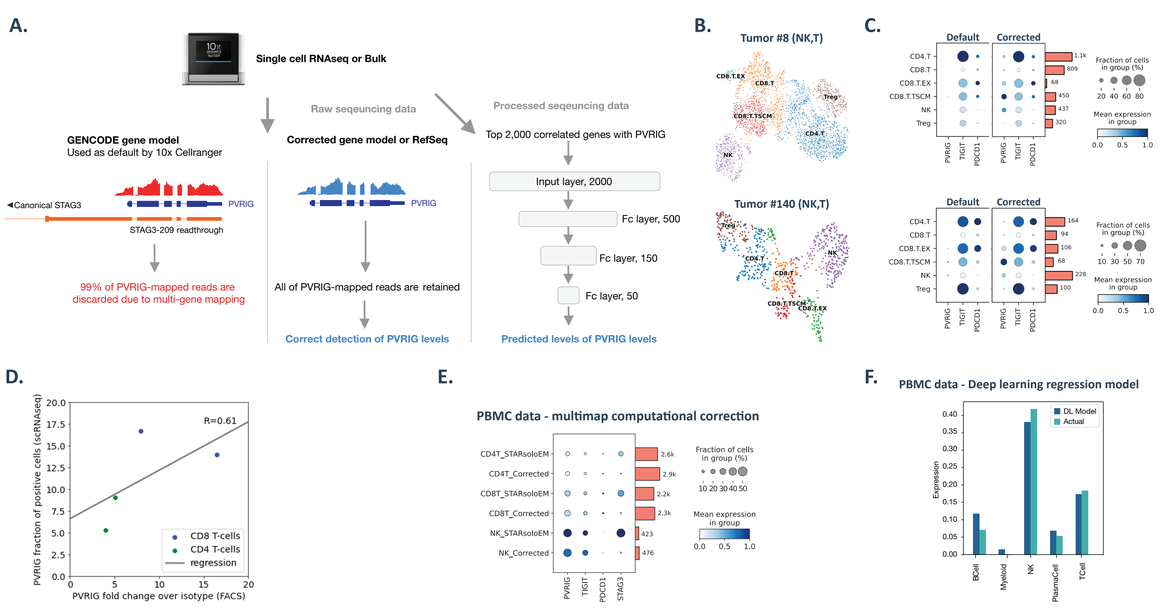

Corrected gene model enables the detection of PVRIG. A. Summarizing illustration; using the GENCODE gene model reads are discarded due to multi-mapping, following the correction of the gene model, or via application of internally trained deep-learning regressor, PVRIG expression is correctly measured. **B.** UMAPs showing the population distribution in two ovarian tumor samples subset for T and NK cells. **C.** Dotplot showing the expression of PVRIG and additional T-cell checkpoints in ovarian tumor samples processed using the default or corrected gene model subset for T and NK cells. Bars indicate number of cells in each sample. **D.** Correlation between PVRIG-positive fraction as measured using FACS (X-axis) to its parallel in the scRNA-seq data following the gene model correction. Linear-regression line is shown in gray as well as the Pearson correlation coefficient. **E.** DotPlot showing the expression of PVRIG, TIGIT, PD-1 and STAG3 in NK/T populations in the PBMC10K dataset processed using the corrected gene model or using STARsolo-EM method. **F.** Barplot showcasing the performance of the deep-learning regression model, trained in-house to predict the levels of PVRIG from processed data. The graph shows the mean expression in different cell populations in the actual data and that predicted by the model.

Gene model correction allows the study of PVRIG in tumor samples, highlighting unique association with Tscm cells and tumor reactive Tscm

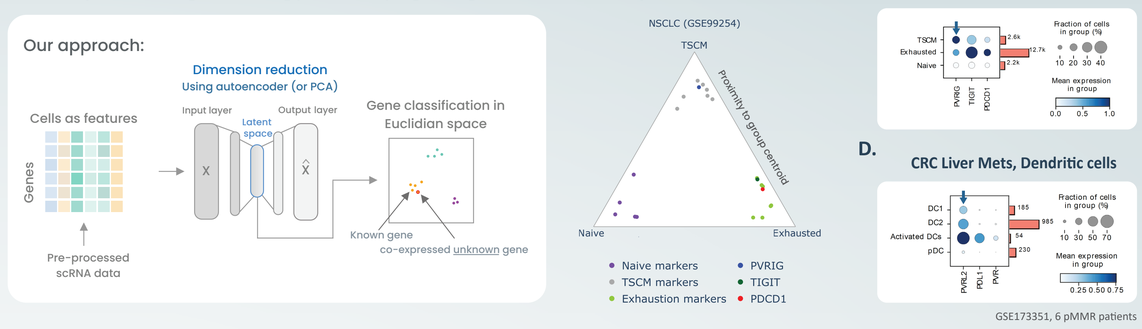

GSE173351, 6 pMMR patients

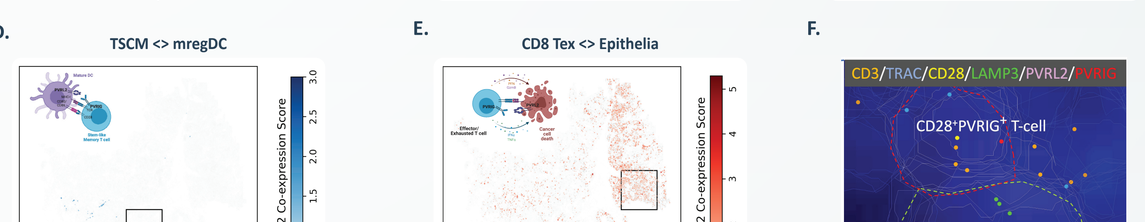

GSE167036 Primary breast cancer

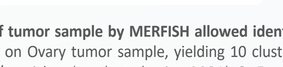

Analysis of scRNA data using the corrected model supported DNAM-1 MOA and differentiation of PVRIG expression vs TIGIT A. Our approach to find co-expressed genes is based on generating custom dimension reduction using deep-learning approach or PCA. **B.** Ternary plot showing the proximity of PVRIG, TIGIT and PD1 (PDCD1) to cell-state centroids, showing PVRIG is associated with Tscm state while the other checkpoints are associated with an exhausted state. **C.** DotPlot showing the expression of PVRIG, TIGIT and PD-1 in CD8 cells isolated from CRC liver mets. PVRIG shows dominant expression on Tscm compared to TIGIT and PD1 **D.** Dotplot showing the expression of corresponding ligands in dendritic cells from the MSS CRC liver mets. Dominant PVRL2 expression is observed on DCs compared to PVR and PDL1. **E.** The activity of PVRIG in Tscm cells is further supported by single-cell TCR analysis. We identified expanded T-exhausted (Tex) cells (with more than 5 cells per clones), indicating they likely antigen specificicity. These clones shared clonal identity with Tscm cells expressing PVRIG, suggesting that inhibiting PVRIG may increase the number of tumor-reactive cells.

Spatial transcriptomics analysis shows distinct PVRIG interactions in ImmuAg versus tumor regions, shedding light on its MOA

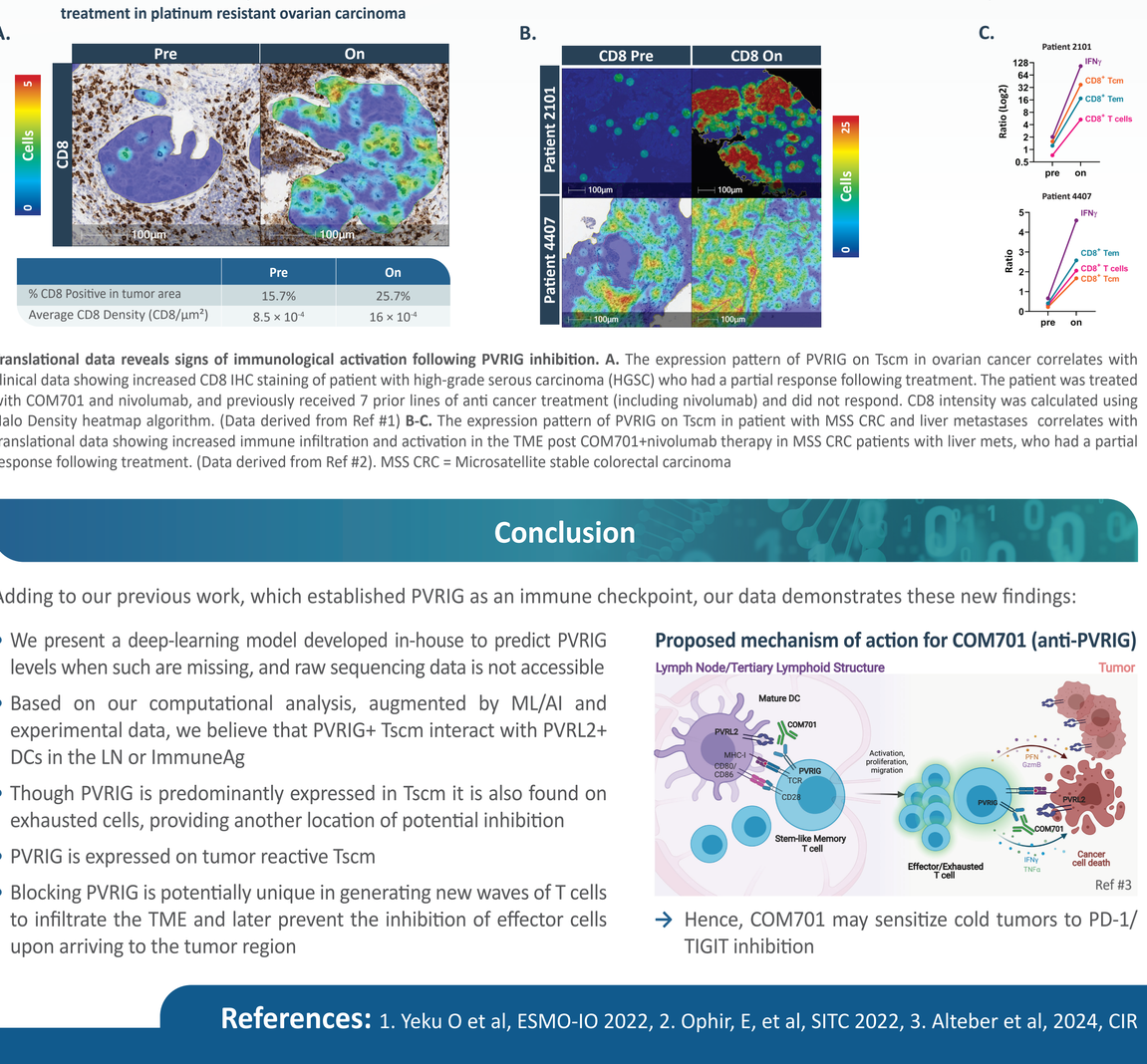

Analysis of tumor sample by MERFISH allowed identification of cellular composition in Immune Aggregates and spatial interaction of PVRIG/PVRL2. A. Cell niche analysis, conducted on Ovary tumor sample, yielding 10 clusters with unique spatial co-localization of different cell populations **B.** Summary network of the distances between cell-types and/or niches (conducted using SOPA) **C.** Focus on the location of immune aggregate niche and inflamed epithelia containing Tex cells. **D.** Spatial ligand-receptor analysis between Tscm expressing PVRIG and neighboring mregDC expressing PVRL2 (NECTIN2) **E.** Spatial ligand-receptor analysis between Tex expressing PVRIG and neighboring Epithelia expressing PVRL2. **F.** CD28+CD8+ T-cell expressing PVRIG intimately interacts with LAMP3+ PVRL2+ DC in the ImmuAg of a CRC patient. Thus, PVRIG inhibition has potential to activate both Tscm in the ImmuAgg to generate waves of Tex and enable them to act against the tumor.A,D,E were conducted using Monkeybread package

Translational data from PVRIG inhibition in clinical studies demonstrates immune activation

Increased CD8+ T cell infiltration post COM701 and nivolumab treatment in platinum resistant ovarian carcinoma

COM701+ nivolumab combination induces TME immune modulation in patients with MSS CRC

	Pre	On
% CD8 Positive in tumor area	15.7%	25.7%
Average CD8 Density (CD8/µm²)	8.5×10^{-4}	16×10^{-4}

Translational data reveals signs of immunological activation following PVRIG inhibition. A. The expression pattern of PVRIG on Tscm in ovarian cancer correlates with clinical data showing increased CD8 IHC staining of patient with high-grade serous carcinoma (HGSC) who had a partial response following treatment. The patient was treated with COM701 and nivolumab, and previously received 7 prior lines of anti cancer treatment (including nivolumab) and did not respond. CD8 intensity was calculated using Halo Density heatmap algorithm. (Data derived from Ref #1) **B-C.** The expression pattern of PVRIG on Tscm in patient with MSS CRC and liver metastases correlates with translational data showing increased immune infiltration and activation in the TME post COM701+nivolumab therapy in MSS CRC patients with liver mets, who had a partial response following treatment. (Data derived from Ref #2). MSS CRC = Microsatellite stable colorectal carcinoma

Conclusion

Adding to our previous work, which established PVRIG as an immune checkpoint, our data demonstrates these new findings:

- We present a deep-learning model developed in-house to predict PVRIG levels when such are missing, and raw sequencing data is not accessible
- Based on our computational analysis, augmented by ML/AI and experimental data, we believe that PVRIG+ Tscm interact with PVRL2+ DCs in the LN or ImmuneAg
- Though PVRIG is predominantly expressed in Tscm it is also found on exhausted cells, providing another location of potential inhibition
- PVRIG is expressed on tumor reactive Tscm
- Blocking PVRIG is potentially unique in generating new waves of T cells to infiltrate the TME and later prevent the inhibition of effector cells upon arriving to the tumor region

Proposed mechanism of action for COM701 (anti-PVRIG)

→ Hence, COM701 may sensitize cold tumors to PD-1/TIGIT inhibition

References: 1. Yeku O et al, ESMO-IO 2022, 2. Ophir, E, et al, SITC 2022, 3. Alteber et al, 2024, CIR